




# Structural and geochronological constraints from the Drina-Ivanjica thrust sheet (Western Serbia): implications for the Cretaceous–Paleogene tectonics of the Internal Dinarides

Kristóf Porkoláb<sup>1</sup>  · Szilvia Kövér<sup>2</sup> · Zsolt Benkó<sup>3</sup> · Gábor H. Héja<sup>2</sup> · Melinda Fialowski<sup>2</sup> · Balázs Soós<sup>2</sup> · Nataša Gerzina Spajić<sup>5</sup> · Nevenka Đerić<sup>5</sup> · László Fodor<sup>2,4</sup>

Received: 30 April 2018 / Accepted: 26 October 2018

© The Author(s) 2018

## Abstract

We have investigated successive episodes of ocean-continent and continent–continent convergence in Western Serbia (Drina-Ivanjica thrust sheet). The coupled application of structural and petrological analyses with Illite Crystallinity measurements and K/Ar dating has revealed the timing and structural characteristics of multiple regional deformation phases, and allowed us to revise the origin of the different Triassic units outcropping in the study area. D<sub>1</sub> tectonic burial was characterized by anchizone metamorphism, dominantly WNW-verging isoclinal folding (F<sub>1</sub>), and related axial planar cleavage (S<sub>1</sub>) formation in the Paleozoic basement and the stratigraphic cover of the Drina-Ivanjica thrust sheet exposed along the northern rim of this thrust sheet. The timing of D<sub>1</sub> deformation is constrained by K/Ar ages suggesting 135–150 Ma tectonic burial for the Drina-Ivanjica thrust sheet. D<sub>1</sub> deformation and metamorphism is correlated with the closure of the Vardar ocean by top-W to NW ophiolite obduction and the underthrusting of the Adriatic distal passive margin below the oceanic upper plate. Since D<sub>1</sub> structures are lacking in the southern occurrences of Triassic rocks within the study area it is proposed that this Triassic is may not be the original sedimentary cover of the Drina-Ivanjica Paleozoic basement. We propose that this southern Triassic originated from a more external Dinaridic thrust sheet and was transported to its present-day position by a top-NE backthrust presumably during late Early Cretaceous–Paleogene times. Map-scale, NW–SE striking D<sub>2</sub> thrust faults and abundant NW–SE trending F<sub>2</sub> folds observed in all units correspond to the general trend of the Dinaridic orogen and are attributed to the latest Cretaceous–Paleogene collision between Adria and Europe. Regional Latest Cretaceous–Paleogene shortening was followed by strike-slip tectonics (N–S shortening and perpendicular extension) and subsequent Miocene normal faulting in both orogen-parallel and orogen-perpendicular directions driven by slab rollback processes of the Carpathian-Dinaridic realm.

**Keywords** Internal Dinarides · Drina-Ivanjica thrust sheet · Deformation history · K–Ar dating · Obduction · Structural analysis

---

Editorial handling: V. Cvetkovic.

---

✉ Kristóf Porkoláb  
k.porkolab@uu.nl

<sup>1</sup> Department of Earth Sciences, Utrecht University, Budapestlaan 6, 3584 CD Utrecht, Netherlands

<sup>2</sup> MTA-ELTE Geological, Geophysical and Space Science Research Group of the Hungarian Academy of Sciences at Eötvös University, 1/C Pázmány Sétány, Budapest 1117, Hungary

<sup>3</sup> Institute for Nuclear Research of the Hungarian Academy of Sciences, 18/c Bem tér, Debrecen 4026, Hungary

<sup>4</sup> MTA-ELTE Volcanology Research Group, 1/C Pázmány Sétány, Budapest 1117, Hungary

<sup>5</sup> Faculty of Mining and Geology, University of Belgrade, Djušina 7, Belgrade, Serbia

## 1 Introduction

Emplacement of oceanic crust on top of continental margins has been an object of particular interest since the observation of the large volumes of ophiolitic complexes exposed in Eurasia (Goffé et al. 1988; Robertson 2004). The understanding of ophiolite obduction has been improved by contributions from analogue (Agard et al. 2014) and numerical (Duretz et al. 2016) experiments, as well as integrated studies (Jolivet et al. 2015). Less is known about the structural evolution of the continental lower plate in obduction systems. How can we trace the record of tectonic burial in the underthrust continental margin? How can we distinguish between the geological record of underthrusting below the ophiolite and a following continental collision phase? How does deformation propagate from the subducting oceanic plate towards the extended passive margin? A suitable place to investigate these questions is the area of Internal Dinarides, where the former Adriatic continental margin—that structurally underlies the ophiolitic nappe of the former Vardar ocean—is exposed in tectonic windows (Bernoulli and Laubscher, 1972; Schmid et al. 2008). The obduction of the Dinaridic (Western Vardar) ophiolites was preceded by intra-oceanic subduction (e.g. Dilek et al. 2007; Maffione et al. 2015) occurring between 174 and 157 Ma according to ages derived from metamorphic soles of the ophiolitic nappe(s) (Dimo-Lahitte et al. 2001; Šoštarić et al. 2014). Intra-oceanic subduction was followed by obduction onto the continental margin which resulted in regional deformation and locally also metamorphism in the Internal Dinarides (e.g. Borojević et al. 2012; Schefer 2012). Based on stretching lineations and associated shear sense indicators, the tectonic transport direction of the ophiolites was top-WNW during obduction (Carosi et al. 1996; Karamata et al., 2000; Schmid et al. 2008; Schefer 2012). To separate the deformation of the lower plate related to ophiolite emplacement from younger collision-related deformation, a clear view on the deformation history is fundamental. The Internal Dinaric structural units like the Studenica or Kopaonik witnessed strong metamorphic overprint due to the Maastrichtian-earliest Paleogene collision between Adria and Europe (Ustaszewski et al. 2009; Schefer 2012) which substantially obliterated the traces of Late Jurassic–Early Cretaceous tectonometamorphic events. We focus on the Drina-Ivanjica thrust sheet, where the conditions of the Cretaceous–Paleogene tectonic evolution are poorly understood. Moreover, the geological record of Late Jurassic–Early Cretaceous tectonometamorphic events are, presumably, less obliterated than in other Internal Dinaric units (Milovanović 1984; Chiari et al. 2011).

We present the result of a field study supplemented by K/Ar dating and Illite Crystallinity measurements, which provides structural and time constraints regarding the Cretaceous–Paleogene evolution of the Drina-Ivanjica thrust sheet. Our study separates deformational structures linked to the underthrusting below the Western Vardar ophiolites from structures attributed to Adria-Europe collision and post-collisional evolution of the area. Distinction between metamorphic and non-metamorphic units as well as units which have or have not been affected by crystal plastic deformation allows the re-interpretation of the origin of Triassic sequences outcropping near the Paleozoic core of the Drina-Ivanjica thrust sheet. Mapping of fault patterns and paleostress analysis furthermore reveal characteristics of the Paleogene–Neogene tectonic evolution of the area.

## 2 Geological setting

The Dinarides are a mountain belt which has been shaped during the Alpine tectonic cycle as a result of the convergence of the Eurasian and Africa-derived plates. The present-day SW-verging nappe stack (Fig. 1) records the opening and closure of either one single branch of Neotethys (Bernoulli and Laubscher 1972; Schmid et al. 2008; Bortolotti et al. 2013) or alternatively, multiple oceanic branches (Dimitrijević 1982; Karamata and Krstić 1996; Karamata 2006). A substantial number of arguments has been published during the last decade supporting the single-Neotethys ocean model, which provides the simplest solution for the geodynamic evolution of the region (e.g. Gawlick et al. 2008; Schmid et al. 2008; Chiari et al. 2011; Schefer 2012; Bortolotti et al. 2013). According to this model, the Adria-derived tectonic units (Adriatic basement and Mesozoic sedimentary cover sequences) structurally underlie the obducted Jurassic ophiolites which originated from a single Vardar/Neotethys ocean and were obducted westward in Late Jurassic–Early Cretaceous times (Fig. 1). Ophiolite emplacement was followed by Early Cretaceous metamorphism and deformation in the Internal Dinarides (Jadar-Kopaonik and Drina-Ivanjica thrust sheets, see Fig. 1) suggesting that the Adriatic margin was tectonically buried due to ophiolite obduction (Milovanović 1984; Milovanović et al. 1995; Tomljenović et al. 2008; Schefer 2012; Toljić et al. 2013). The Jurassic–Early Cretaceous tectonic contacts were substantially overprinted by the Late-Cretaceous–Paleogene collision of Adria and Eurasia following the final closure of the remnants of Neotethys referred to as Sava (Ustaszewski et al. 2009, 2010). Collision resulted in the formation of the SW-verging Dinaridic nappe stack which largely defines the presently used structural subdivision of the Dinarides (Fig. 1) (Schmid

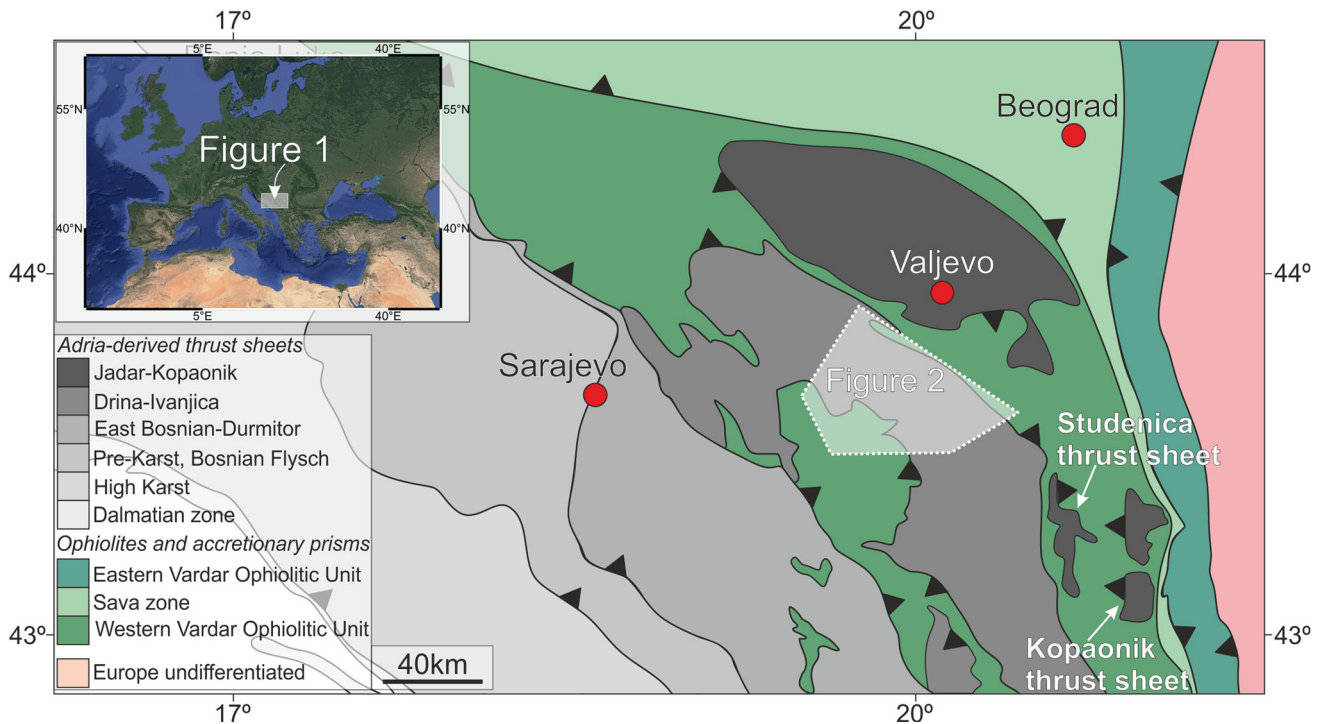


**Fig. 1** Tectonic map of the Internal Dinarides modified after Schmid et al. (2008). The location of the study area is outlined by the white polygon (see Fig. 2)

et al. 2008). The structure of the Dinarides was further modified by Paleogene–Neogene strike-slip tectonics (e.g. Csontos et al. 2004; Ilic and Neubauer 2005) and the formation of a Neogene extensional basin system due to slab-rollback processes (e.g. Ustaszewski et al. 2010; Matenco and Radivojevic 2012; Toljic et al. 2013; Andric et al. 2017).

## 2.1 Geology of the study area

The study area exposes the Western Vardar ophiolites and Adria-derived Paleozoic–Mesozoic sequences, which together form the Drina-Ivanjica thrust sheet (Figs. 1 and 2) (Milovanovic 1984; Brkovic et al. 1977; Mojsilovic et al. 1977; Milovanovic 1984; Olujic and Karovic 1986; Schmid et al. 2008; Chiari et al. 2011). According to previous works, the Paleozoic of the Drina-Ivanjica thrust sheet is displayed in the core of a NW–SE trending anticline, and its Triassic sedimentary cover is found along both the NE and SW limbs of the anticline (Milovanovic 1984; Schmid et al. 2008; Chiari et al. 2011). Further in the text the Triassic units exposed along the NE and SW limbs of the Drina-Ivanjica anticlinal core exposing the Paleozoic are referred to as Northern and Southern Triassic units, respectively.

The Drina-Ivanjica Paleozoic basement largely consists of Carboniferous metasandstone, metaconglomerate, phyllite, slate, and marble (Brkovic et al. 1977; Mojsilovic et al.

1977; Olujic and Karovic 1986; Chiari et al. 2011; age constrained by Stojanović and Pajić, 1966–71). The Carboniferous rocks have experienced low-grade metamorphism and multiple phases of deformation (Milovanovic 1984; Djokovic 1985; Trivic et al. 2010). However, the timing of deformation events is still unclear: the only available age constraints for the metamorphism of the Drina-Ivanjica Paleozoic are white mica K/Ar ages that range between 160 and 179 Ma (Milovanovic 1984) and unpublished K/Ar ages between 129 and 139 Ma [Lovrić, personal communication, reported by Milovanovic (1984)]. Outside the study area, older Paleozoic rocks [Cambrian–Silurian based on phytoplanktons and spores, Ercegovac (1975)] with higher metamorphic grade are also found within this thrust sheet; the age of this metamorphism is assumed to be Variscan (Milovanovic 1984).

Until now the Northern and Southern Triassic units were mapped as one and the same unit considered to represent the original sedimentary cover of the Drina-Ivanjica Paleozoic (Brkovic et al. 1977; Mojsilovic et al. 1977; Olujic and Karovic 1986; Chiari et al. 2011). In the Southern Triassic unit the stratigraphic succession ranges from Lower Triassic to Lower Jurassic, while the Northern Triassic unit comprises a Lower to Middle Triassic succession (Fig. 2a). The lithological succession of the two units is similar and is generally described together (Chiari et al. 2011; Kovács et al. 2011). The Lower Triassic is characterized by continental siliciclastic rocks

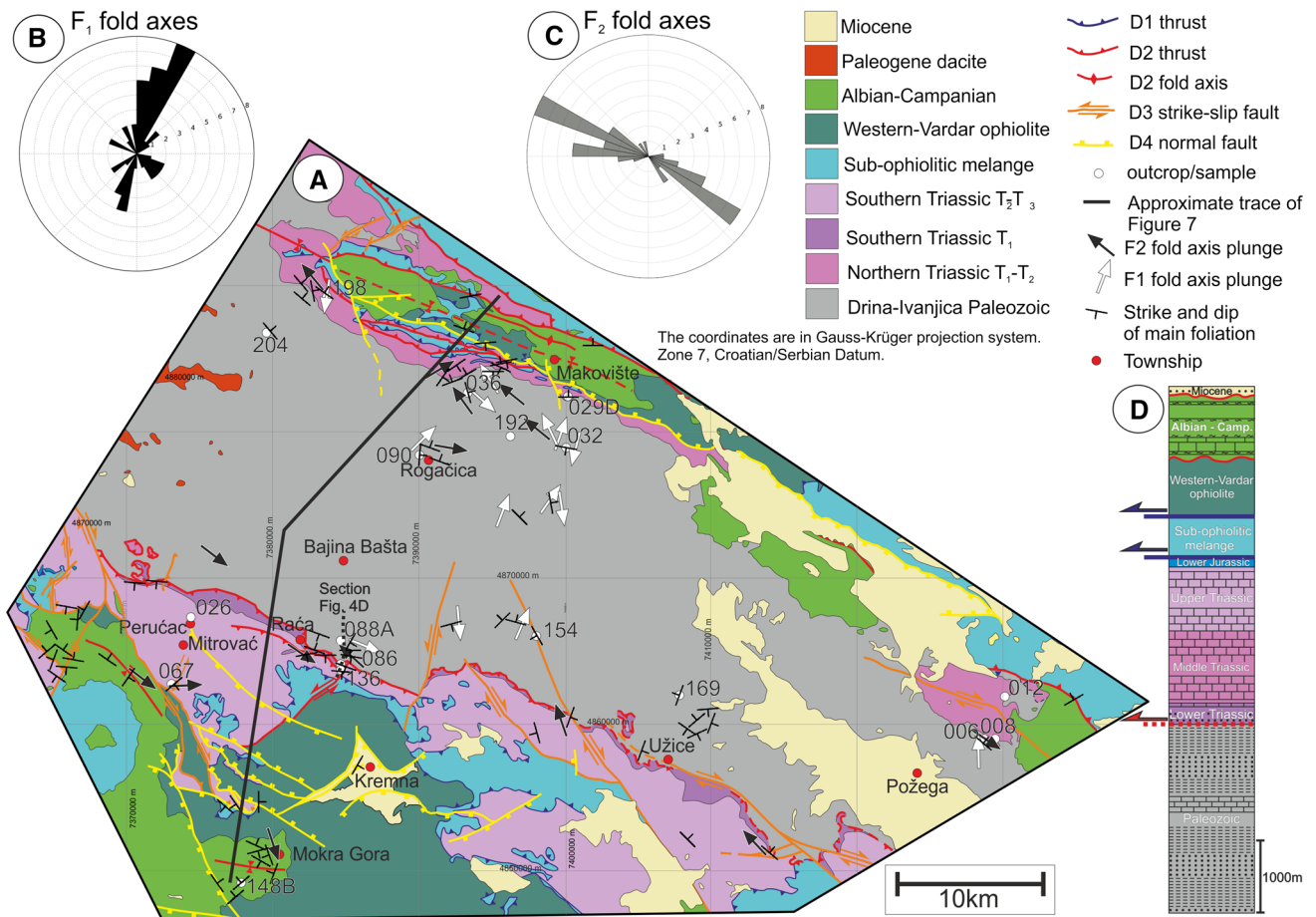


**Fig. 2** **a** Geological map of the study area based on the geological maps of former Yugoslavia, sheets Višegrad, Ljubovija, Valjevo, Čačak, Titovo Užice (Mojsilovic et al. 1972; Kubat et al. 1976; Brkovic et al. 1977; Mojsilovic et al. 1977; Olujic and Karovic 1986; Osnovna Geološka Karta SFRJ) and Chiari et al. (2011). **b** Rose

diagram of the strike of  $F_1$  fold axis orientation. Number of measured data for each azimuth slice is indicated. **c** Rose diagram of the strike of  $F_2$  fold axis orientation. Number of measured data for each azimuth slice is indicated. **d** Simplified stratigraphic column of the study area

(conglomerates and sandstones) that grade into a mixed siliciclastic-carbonate marine succession in the upper part. The Middle Triassic exhibits 400–600 m thick Anisian Gutenstein- and Steinalm-type limestones followed by the red, nodular, hemipelagic Han Bulog Formation (Chiari et al. 2011; Kovács et al. 2011). The Middle-Late Triassic carbonate platform evolution is evidenced by the Wetterstein- and Dachstein-type limestones, which reach a thickness of 700 m (Brkovic et al. 1977; Mojsilovic et al. 1977; Olujic and Karovic 1986; Kovács et al. 2011). The Southern Triassic unit exhibits minor patches of Lower Jurassic hemipelagic limestones, which are the youngest preserved sediments of the passive Adriatic margin exposed in the study area. In the Drina-Ivanjica thrust sheet outside the study area Lower and Middle Jurassic cherts have been described implying a substantial deepening of the Adriatic margin prior to ophiolite obduction (Djerić et al. 2007; Gawlick et al. 2009; Chiari et al. 2011).

The Western Vardar Ophiolitic Unit of the Drina-Ivanjica thrust sheet structurally overlies these passive margin successions and consists of the sub-ophiolitic melange and the ophiolites (Fig. 2a, d) (Schmid et al. 2008). The Middle Jurassic (Gawlick et al. 2009) sub-ophiolitic melange consists of (1) fine-grained siliciclastic matrix accumulated in a deep basin formed ahead of advancing ophiolitic thrust sheet that comprises blocks of various size and lithology; and (2) material scraped off from the footwall of the ophiolite thrust (Adriatic units) (Bortolotti et al. 1996; Chiari et al. 2011). WNW-ESE trending stretching lineations and top-WNW kinematic indicators in the sub-ophiolitic melange imply top north-west tectonic transport of the ophiolitic thrust sheet (Carosi et al. 1996; Schmid et al. 2008; Schefer 2012).

The ophiolites structurally overlie the sub-ophiolitic melange and are made up of Upper Jurassic lherzolite, harzburgite, serpentinite, and mylonitic amphibolite in the metamorphic sole of the ophiolite (the age of the ophiolites

is constrained by radiometric dating in Spray et al. 1984; Dilek 2008; Ustaszewski et al. 2009). The geochemical signal of parts of the mantle rocks implies supra-subduction zone (SSZ) origin of the obducted succession (Bazylev et al. 2009; Chiari et al. 2011). The metamorphic sole formed during intra-oceanic subduction pre-dating obduction. Dating of the metamorphic soles implies that the formation of the Late Jurassic SSZ ophiolites was immediately followed by intra-oceanic subduction within young oceanic lithosphere (Dimo-Lahitte et al. 2001; Maffione et al. 2015).

On their top ophiolites and underlying units of the Drina-Ivanjica thrust sheet are truncated by an erosional unconformity of mid-Cretaceous in age (Fig. 2d) (Pejovic and Radoicic 1971; Mojsilovic et al. 1972; Kubat et al. 1976; Brkovic et al. 1977; Mojsilovic et al. 1977; Olujic and Karovic 1986). This unconformity truncates the Drina-Ivanjica thrust sheet at all levels, i.e. from the Western Vardar ophiolites to the Paleozoic basement (Fig. 2). The Drina-Ivanjica Paleozoic basement is transgressed along a younger unconformity by Upper Cretaceous („Senonian”) sediments in the core of the Drina-Ivanjica antiform.

Laterites and fluvial clastics seal the older unconformity and are followed by Albian-Cenomanian mixed siliciclastic-carbonate ramp succession (Pejovic and Radoicic 1971). These strata are conformably topped by Turonian-Santonian rudist limestones and by a Cretaceous–Paleogene flysch succession documented outside the study area (Brkovic et al. 1977; Chiari et al. 2011). The youngest formations of our study area are Miocene siliciclastic rocks found in small basins (Fig. 2a) (Brkovic et al. 1977; Mojsilovic et al. 1977; Osnovna Geološka Karta SFRJ).

### 3 Analytical methods

#### 3.1 Illite crystallinity

In the very low-grade metamorphic zone a widely accepted and applied method is the illite “crystallinity” method introduced by Kübler (1966, 1968), based on X-ray powder diffraction (XRPD). This work presents Kübler Indices (KI) data in order to characterize the metamorphic grade of different formations.

X-ray diffraction (XRD) measurements of the clay fraction (< 2  $\mu\text{m}$ ) were carried out using a Rigaku Miniflex diffractometer with  $\text{CuK}\alpha$  radiation at 40 kV and 15 mA in the laboratory of the Institute for Geological and Geochemical Research of the Hungarian Academy of Sciences. Clay minerals were identified by XRD diagrams obtained from parallel-oriented specimens. Diagnostic treatments were carried out for the identification and characterization of clay minerals. Ethylene glycol solvation at 60 °C

overnight was used for the detection of swelling clay minerals and mixed layer clay minerals.

The calibration procedure of the phyllosilicate “crystallinity” index measurements was carried out against that of Kübler’s laboratory using 0.25 and 0.42  $\Delta^2\theta$  as the anchizone boundary values (for details see Árkai and Ghabrial 1997). The illite “crystallinity” (KI = Kübler index) boundaries of the anchizone correspond to 0.25 and 0.42  $\Delta^2\theta$  in the present work. On the basis of this calibration, using also linear regression equations between KI and chlorite “crystallinity” (ChC) indices (Árkai et al. 1995), the actual ranges of the anchizone are 0.26–0.38  $\Delta^2\theta$  for ChC (001), and 0.24–0.30  $\Delta^2\theta$  for ChC (002). These entire boundary values refer to air dried (AD) mounts.

#### 3.2 K/Ar dating

In order to determine the timing of metamorphism and deformation, the K/Ar method was applied. Experiments were carried out on both 1 and 2  $\mu\text{m}$  fractions of illite in order to constrain the fraction size-dependence of the results. The separated size fractions were analyzed by the K–Ar method (Balogh 1985) in the K–Ar laboratory of the Institute for Nuclear Physics of the Hungarian Academy of Sciences in Debrecen. The potassium content was measured on 50 mg sample aliquots after dissolution by HF and  $\text{HNO}_3$ , by a Sherwood-400 type flame spectro-photometer with an accuracy better than  $\pm 1.5\%$ . The potassium content of the samples might vary due to different ratios of illite/chlorite in the samples (Table 2). Separated mineral sample splits were subjected to heating at 100 °C for 24 h under vacuum to remove atmospheric Ar contamination that adsorbed on the surface of the mineral particles during sample preparation. Argon was extracted from the minerals by fusing the samples by high frequency induction heating at 1300 °C. The released gases were cleaned in two steps in a low-blank vacuum system by St-700 and Ti-getters. The isotopic composition of the spiked Ar was measured by a Nier-type mass spectrometer. The atmospheric Ar ratio was analyzed each day during the measurement period and averaged  $295.6 \pm 1.85$  ( $1\sigma$ ) for 60 independent determinations. All isotope measurements were corrected by the atmospheric  $^{40}\text{Ar}/^{36}\text{Ar}$  ratios determined on the day of the analysis. The accuracy and reproducibility of the isotope ratio measurements were periodically controlled by the Rodina 2/65 internal standard for which the radiogenic  $^{40}\text{Ar}$  content averaged  $13.72 \pm 0.12$  ( $2\sigma$ )  $\times 10^{-6} \text{ cm}^3 \text{ g}^{-1}$  STP after five independent determinations. The recommended value is  $13.71 \times 10^{-6} \text{ cm}^3 \text{ g}^{-1}$ . The decay constants recommended by Steiger and Jäger (1977), were used for age calculation with an overall error of  $\pm 2\%$ .

## 4 Results

### 4.1 Structures and deformation phases

Field work was carried out in the study area in order to determine the superposition of deformation events in the different geological units. As a result of multi-scale structural analysis, an overview of the deformational structures is presented below in a relative chronological order.

D<sub>1</sub> structures represent the only ductile (crystal plastic) structures found in the Paleozoic and in the Northern Triassic unit of the study area (Figs. 2, 3). Dynamic recrystallization of calcite and quartz was observed in thin section (Fig. 3) in association with numerous tight to isoclinal F<sub>1</sub> folds in metasedimentary rocks (Figs. 2, 3). F<sub>1</sub> folding was accompanied by the formation of a penetrative axial planar cleavage (S<sub>1</sub>), which is pervasive in the slaty-phyllic Paleozoic rocks, and less pronounced in the carbonate-rich Northern Triassic unit. The prevailing NNE–SSW trend of the measured F<sub>1</sub> fold axes suggests an ESE–WNW shortening direction (Fig. 2b), while the commonly observed asymmetry of F<sub>1</sub> folds suggests top–WNW tectonic transport direction for D<sub>1</sub> phase. Transposition by solution and neo-crystallization of S<sub>0</sub> bedding due to intense D<sub>1</sub> deformation was frequently observed (Fig. 3). Structures of D<sub>1</sub> phase were not observed neither in the Southern Triassic unit which preserves intact fossils and carbonate texture (Fig. 3f) nor in the Cretaceous sedimentary sequences.

The D<sub>2</sub> deformation phase is characterized by gentle to tight folding of the S<sub>1</sub> main foliation and S<sub>0</sub> bedding, and by NW–SE striking reverse faults (Fig. 4a, b). D<sub>2</sub> structures affect all stratigraphic units of the study area from the Paleozoic basement all the way to the Upper Cretaceous (Fig. 2a). The trend of F<sub>2</sub> fold axes and D<sub>2</sub> thrusts implies a NE–SW shortening direction for the D<sub>2</sub> phase (Fig. 2c). The vergence of D<sub>2</sub> thrusts and asymmetric F<sub>2</sub> folds are top–SW in the NE part of the study area, but top–NE in the SW part of the study area (Figs. 2a, 4 and 7). No dynamic recrystallization of minerals was observed associated with D<sub>2</sub> structures. Microscale deformation mechanisms like calcite twinning and dissolution were occasionally observed in the hinge zone of F<sub>2</sub> folds (Fig. 3f). Brittle reverse faults and F<sub>2</sub> folds are in most cases linked, suggesting that fault-related folding was the predominant mechanism during the D<sub>2</sub> phase. No penetrative planar structure has been observed to be associated with the D<sub>2</sub> phase except for the rare occurrence of a S<sub>2</sub> crenulation cleavage (folding the S<sub>1</sub> axial plane cleavage) in carbonate layers of the Paleozoic and in the Northern Triassic unit.

D<sub>3</sub> structures are dominantly strike-slip faults, which cut D<sub>2</sub> thrusts (Fig. 2a). These are mostly NNW–SSE striking dextral and subordinately NE–SW striking sinistral faults. A large population of measured mesoscale strike-slip faults show a pattern similar to the map-scale structures. Inversion of fault-slip data (for methodology see Angelier 1984) implies roughly N–S compression and E–W extension for D<sub>3</sub> structures (Fig. 5).

D<sub>4</sub> structures are map- and outcrop-scale normal faults that in some cases cut the D<sub>3</sub> strike-slip faults (Fig. 2a). Superposition of slickenside lineation observed and measured at the outcrops (for locations see Fig. 5) also suggests post-D<sub>3</sub> normal faulting. Extension directions derived from the normal fault dataset are both NE–SW and NW–SE (Fig. 5). No clear evidence has been found clarifying the relative order of the NE–SW and NW–SE extension; they might be partly or entirely simultaneous.

### 4.2 Illite crystallinity measurements

The results of the measurements are shown in Table 1. The Paleozoic samples fall into the range of high-temperature anchizonal metamorphism (range of  $0.25 < KI < 0.3$ ; samples 006C, 154, 203 and 090), and low-temperature anchizonal metamorphism (range of  $0.3 < KI < 0.42$ ; samples 006E and 036D). One sample from the Lower Triassic of the Northern Triassic unit (012A) shows low-temperature anchizonal metamorphism. One sample from the Lower Triassic of the Southern Triassic unit (086A) shows a non-metamorphic (diagenetic) value. In case of this sample, the presence of smectite might have disturbed the measurement. XRPD analysis detected paragonite in case of samples: 006E, 036D, 090, 154, and 203. Paragonite is an index mineral for anchizonal metamorphism in pelitic rocks, thus its presence supports the results of the Illite Crystallinity measurements (Frey 1970).

### 4.3 K/Ar measurements

The results of K/Ar measurements of 15 samples are presented in Table 2. The dominant range of K/Ar ages in the samples of the Drina-Ivanjica Paleozoic and the Northern Triassic unit is  $\sim 135$ – $175$  Ma. Measurements on both 1 and 2  $\mu\text{m}$  fractions were carried out on five samples (Table 2; Fig. 6a). The results of these experiments exhibit a clear difference between the ages of the two fractions: four out of the five samples have significantly younger 1  $\mu\text{m}$ -fraction ages compared to the 2  $\mu\text{m}$ -fraction ages, while in case of sample 29D the two fractions yielded similar ages (Fig. 6a). The  $\sim 61$  Ma, 1  $\mu\text{m}$ -fraction age of sample 192 (Table 2) is an exception from the dominant Late Jurassic–Early Cretaceous age population.

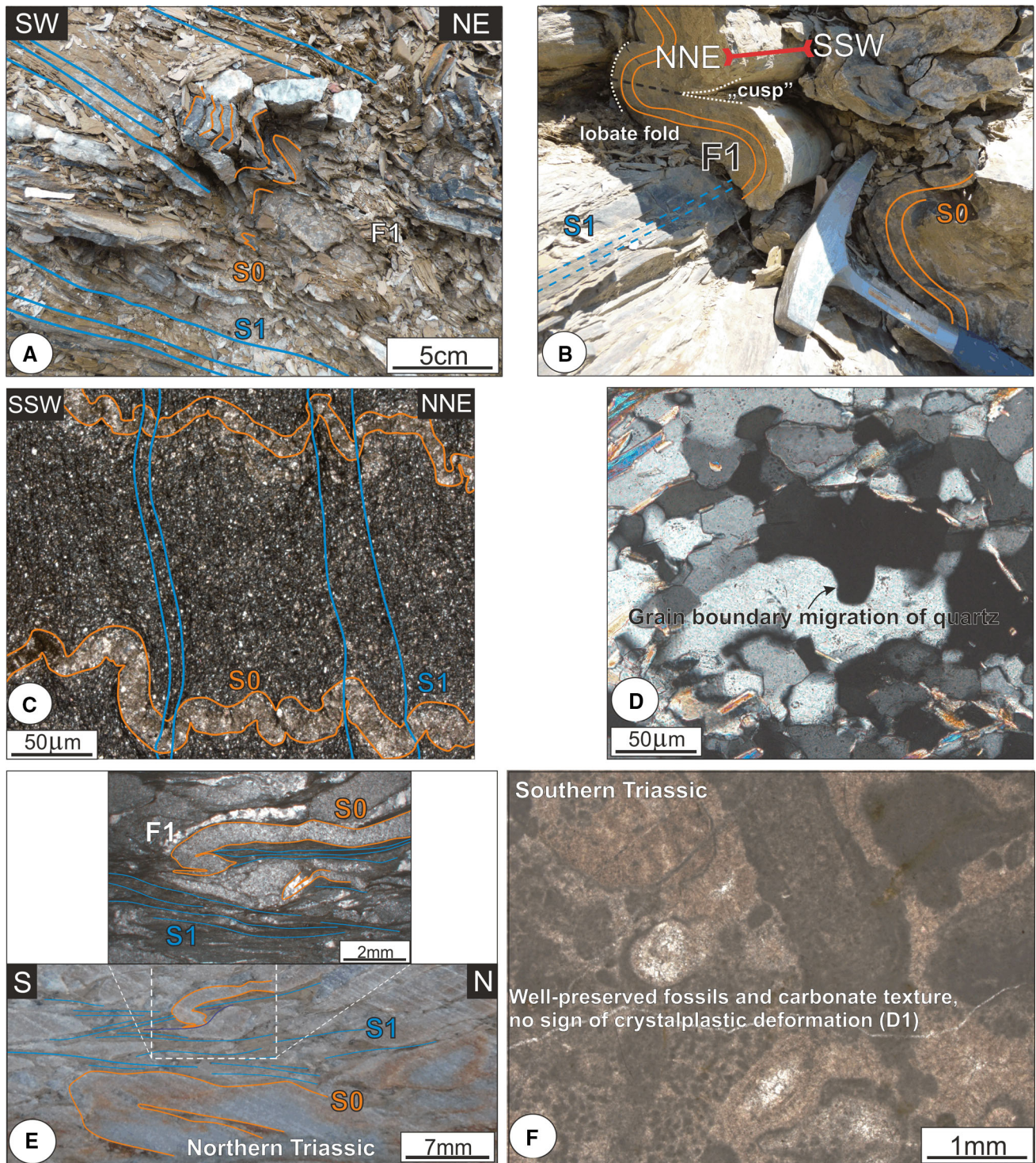


**Fig. 3** Photographs and interpretations of key observations. The stratigraphic younging direction is upwards in all pictures. For outcrop locations see Fig. 2a. **a** Remnants of tight to isoclinal  $F_1$  folds and penetrative  $S_1$  axial planar cleavage in the Drina-Ivanjica Paleozoic (outcrop 006). **b** WNW-verging tight to isoclinal  $F_1$  folds in competent marble layers in the Drina-Ivanjica Paleozoic (outcrop 032). **c** Thin section from outcrop 006 (Drina-Ivanjica Paleozoic) showing buckling of the  $S_0$  bedding plane and related  $S_1$  axial planar

cleavage defined by solution surfaces. **d** Subgrain formation and grain boundary migration of quartz during  $D_1$  phase in thin section from outcrop 169 (Drina-Ivanjica Paleozoic). **e** Tight to isoclinal  $F_1$  folds and related  $S_1$  axial planar cleavage in the Northern Triassic unit at outcrop 198. **f** Thin section from the Southern Triassic unit showing well-preserved carbonate texture and the lack of  $D_1$  deformation structures (outcrop 026)

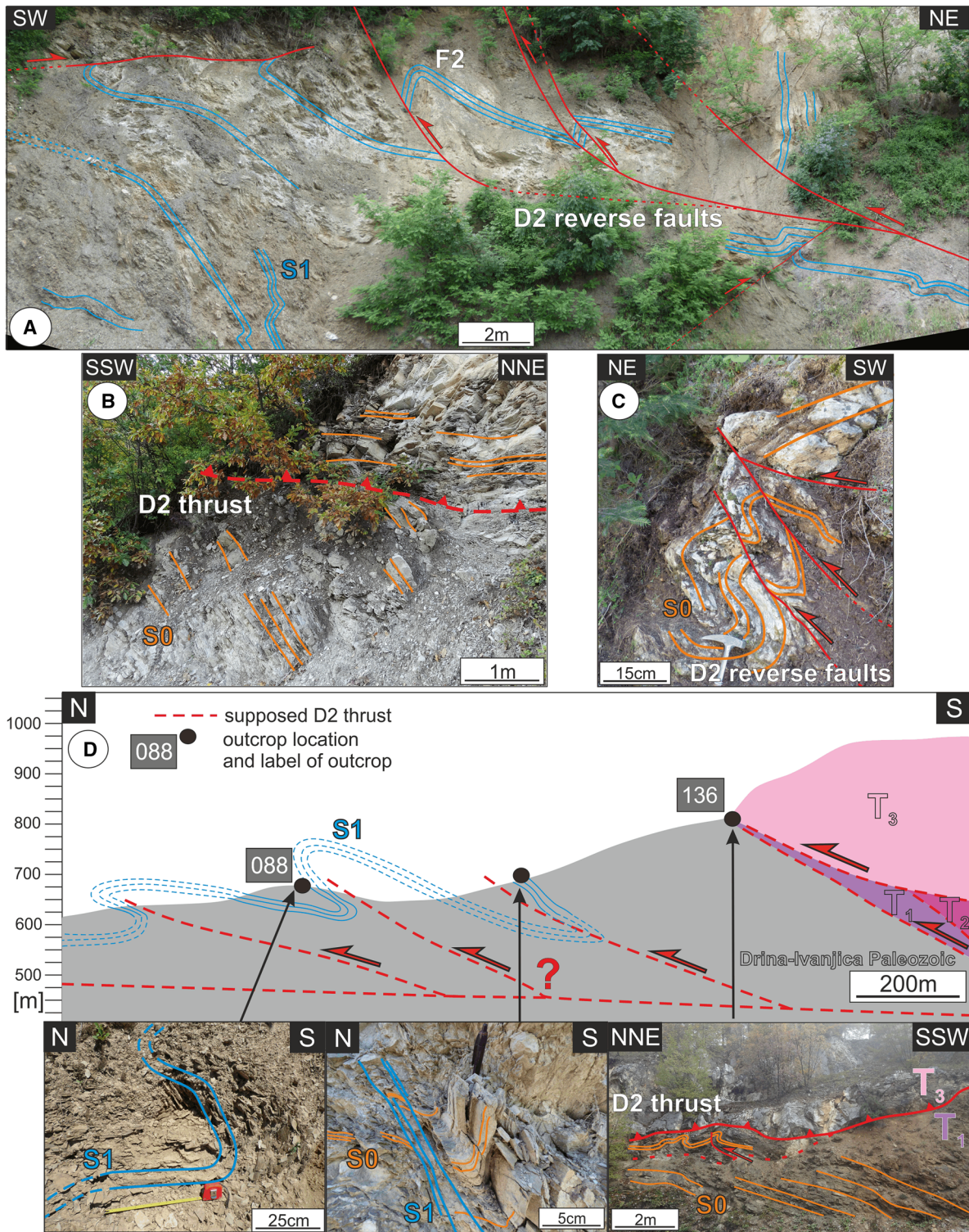


**Fig. 4** Mesoscale D<sub>2</sub> deformation structures. For outcrop locations see Fig. 2a. **a** Southwest-verging D<sub>2</sub> reverse faults and related F<sub>2</sub> folds in the Drina-Ivanjica Paleozoic (outcrop 006). **b** D<sub>2</sub> thrust fault (top-SW tectonic transport) in the Albian-Campanian succession at outcrop 148B. **c** Top-NNE D<sub>2</sub> reverse faults and related folds in the Southern Triassic unit (outcrop 067). **d** Geological cross-section at the

boundary between the Drina-Ivanjica Paleozoic and the Southern Triassic unit (for section trace see Fig. 2a) showing the location of the observed structures at a smaller scale (bottom) and our interpretation of the observations. The vergence of folding and thrusting is top-NNE along the section



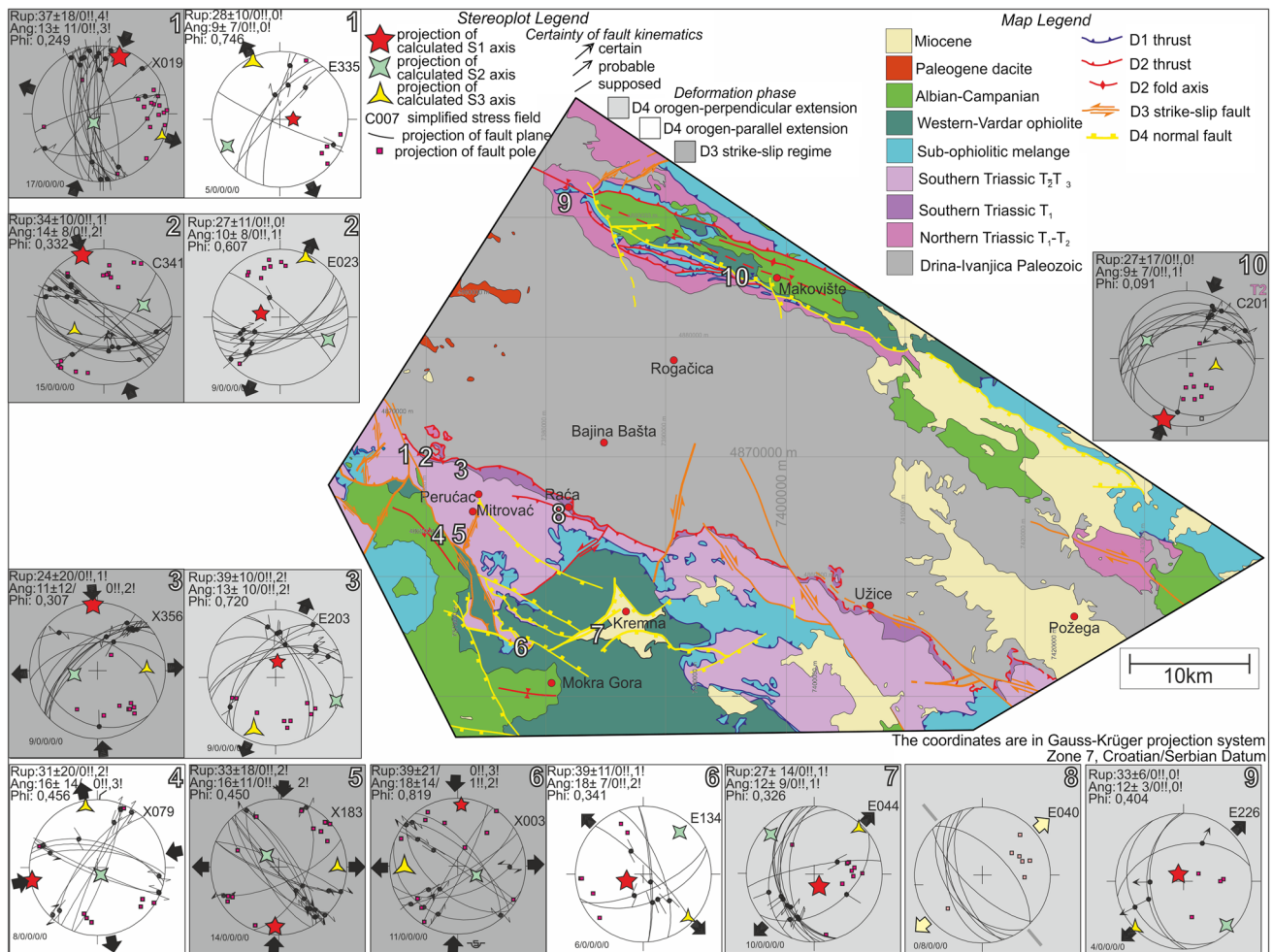


**Fig. 5** Stereographic projections of fault-slip data collected in the study area. The locations of measurements are indicated by the number in the top right corner of the boxes. The data are grouped according to the distinguished deformation phases (D<sub>3</sub> strike-slip faulting, D<sub>4</sub> orogen-perpendicular and orogen-parallel extension). ANG, RUP are the quality indices of the paleostress calculations (for

details see Angelier 1984). ANG: angular difference between the measured striae and the “ideal” striae calculated on the basis of the determined tensor. RUP: difference between the calculated shear stress vector of a particular fault and the absolute value of the vector that is requisite to produce slip on that plane. Phi ( $\Phi$ ) is the ration of stress axes  $(\sigma_2 - \sigma_3)/(\sigma_1 - \sigma_2)$

The 2  $\mu$ m-fraction K/Ar age ( $\sim 198$  Ma) of the sample from the Southern Triassic unit (sample 86A, Table 2) is significantly older than the ages from the other units.

## 5 Discussion

### 5.1 Interpretation of IC and K–Ar data

The interpretation of K–Ar ages measured on illite–K-white mica rich separates is a difficult task, since illite–K-white mica may have formed below and also above the closure temperature of K–Ar system, which is estimated as  $260 \pm 30$  °C for the  $< 2$   $\mu$ m grain size fraction of illite (Hunziker et al. 1987). Detrital illite/sericite/muscovite mixing with authigenic illite can significantly affect the

results of the measurements. However, if the system reached the high-temperature anchizone metamorphic stage, the radiometric clock of the detrital dioctahedral crystals had to be almost completely reset and should indicate the age of metamorphism. The formation of white micas may be a long-lasting process, which can be strongly influenced by the chemical composition of fluids present in the rock (Roberson and Lahann 1981). Moreover, isotopically non-equilibrated detrital micas can be present in metasedimentary rocks, which complicates the interpretation. Being aware of these characteristics of illite formation and the related K/Ar system, it is highly advantageous to apply the Illite Crystallinity and K/Ar method together on the same samples, coupled with a microstructural characterization.

**Table 1** Illite crystallinity (Kübler Index) measurements from the study area

Sample code	Geological unit	Kübler Index (KI)
154	Drina-Ivanjica Paleozoic	0.293
204	Drina-Ivanjica Paleozoic	0.298
012A	Northern Triassic	0.328
036D	Drina-Ivanjica Paleozoic	0.35

KI > 0.42 → diagenetic; 0.3 < KI < 0.42 → low-temperature anchizone; 0.25 < KI < 0.3 → high-temperature anchizone; KI < 0.25 → epizonal metamorphism. For sample locations see Fig. 2a

We examined several samples with both IC and K/Ar methods. The two parameters show a strong correlation. The trend of the regression line (Fig. 6b) implies that the K/Ar ages become younger with a decrease of the KI values. The decrease in KI values means increase in the change of the crystal structures of the K-white mica minerals, which is the result of increasing metamorphic degree. Based on IC measurements (Table 1) and microstructural characterization (Fig. 3), the samples of the Drina-Ivanjica Paleozoic and Northern Triassic unit are affected by anchizonal metamorphism. In the case of such low-grade metamorphic conditions, relatively small (20–40 °C) temperature variations might cause significant changes in the mineral structures considering that the structural development of the K-white mica is a slow and continuously ongoing process in the anchizone (Hunziker et al. 1987). It is likely, that the K/Ar system had not been completely

reset in case of the samples which did not reach the high-temperature anchizone (samples 012, 036), thus resulting in mixed K/Ar ages which are somewhat older than the true age of metamorphism. In contrast, the samples which have reached the high temperature anchizone (samples 154, 203) might indicate the timing of metamorphism (130–145 Ma) more precisely (Fig. 6b).

In case of samples 006E, 008D, 088A, and 192, the measurements of the finer 1 µm fraction gives younger ages compared to the 2 µm fractions of the same samples (Fig. 6a). This implies that the finer fractions are probably less contaminated by inherited material than the coarser fractions, and consists of newly formed white mica crystals. Taking this into account, the likely range for the age of metamorphism in the Drina-Ivanjica Paleozoic and the Northern Triassic unit is ~ 150 to 130 Ma (very Latest Jurassic to Early Cretaceous).

## 5.2 Relation between metamorphism and deformation

Based on microstructures such as subgrain formation and initial grain boundary migration of quartz, and dynamic recrystallization of white mica and calcite (Fig. 3), one can estimate the minimum peak temperature for D<sub>1</sub> to be about 270 °C (Voll 1976). Significantly higher temperature is not probable, since the scarcely observed dynamic recrystallization of quartz represents the feature related to the highest metamorphic alteration visible in the thin sections. This 270 °C temperature estimate is in a good agreement with the Kübler Index values obtained from

**Table 2** K–Ar measurements of 15 samples

Sample code	Geological unit	Fraction (µm)	K (%)	Ar <sub>rad</sub> (× 10 <sup>-5</sup> cm <sup>3</sup> g <sup>-1</sup> )	Age (Ma)	± (Ma)
006E	DI-PZ	2	4.814	3.36869	171.59	4.47
006E	DI-PZ	1	4.005	2.38123	146.81	3.88
008D	N-Tr	2	4.308	2.67731	153.18	3.97
008D	N-Tr	1	5.041	2.77226	136.20	3.66
012A	N-Tr	2	6.478	4.26984	162.06	4.70
029D	N-Tr	2	2.687	1.53757	141.51	5.13
029D	N-Tr	1	3.139	1.82609	143.77	4.23
036D	DI-PZ	2	5.503	3.70623	165.43	4.64
086A	S-Tr	2	4.473	3.64564	198.35	5.58
088A	DI-PZ	2	4.520	3.29494	178.41	5.18
088A	DI-PZ	1	4.140	2.43821	145.48	3.77
192	DI-PZ	2	3.692	2.07668	139.19	4.16
192	DI-PZ	1	3.156	7.6252	61.11	2.20
154	DI-PZ	2	4.186	2.28010	134.95	4.21
204	DI-PZ	2	5.152	2.93744	141.01	4.45

For sample locations see Fig. 2a

DI-PZ Drina-Ivanjica Paleozoic basement, N-Tr Northern Triassic unit, S-Tr Southern Triassic unit

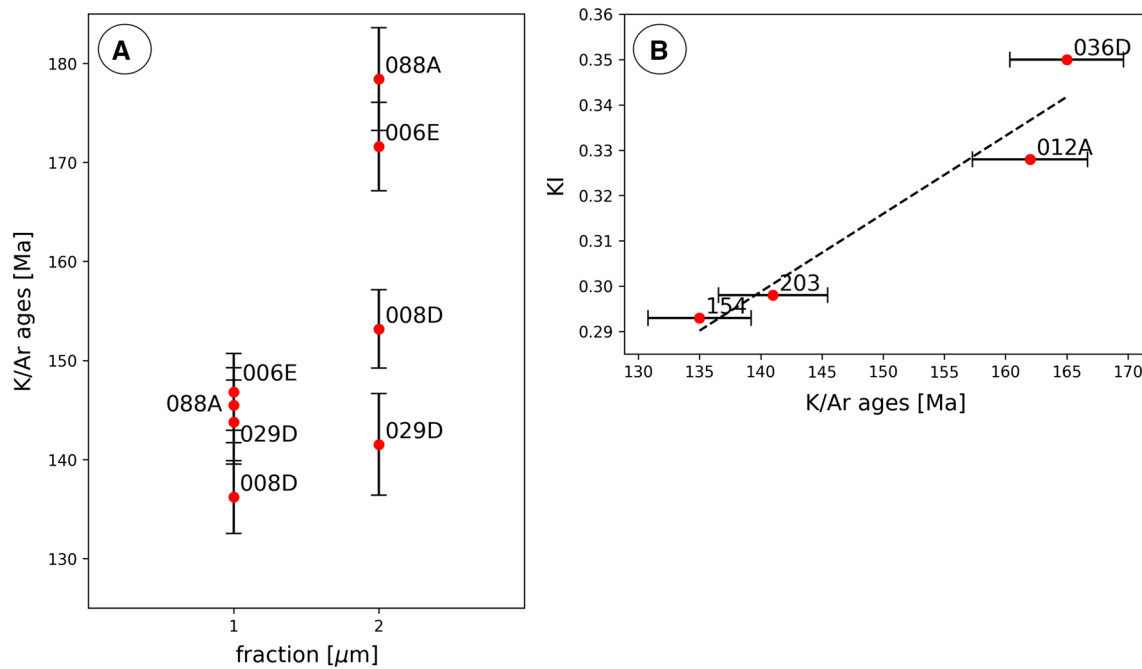


**Fig. 6** **a** Plot showing the influence of illite fraction size on the K/Ar ages. **b** Plot showing the correlation between illite crystallinity (KI values) and K/Ar ages measured on 2  $\mu\text{m}$  illite fractions. For sample locations see Fig. 2a

samples of the Paleozoic and Northern Triassic unit, which all fall in the interval of the anchizone metamorphism. The temperature range of the anchizone is approximately 200–300 °C, wherein the range of high-temperature anchizone is roughly 260–300 °C (Abad 2007). The average of the Kübler Index values of Paleozoic and Northern Triassic samples is 0.299 (Table 1), which is almost exactly the boundary (0.3) between the low- and high-temperature anchizone metamorphism (Table 1). Thus, the average peak temperature reached by these units is likely to be around 260–300 °C based on this measurement. Calculating with an average (approximately 3 °C/100 m) geothermal gradient this temperature would mean 9–10 km depth for the deepest burial of the Drina-Ivanjica thrust sheet. Based on our K/Ar measurements, the age of the anchizone metamorphism is estimated to be 130–150 Ma.

Since  $D_1$  is the only observed crystal plastic deformation phase within our study area, and the estimated temperature based on  $D_1$  microstructures is in a good agreement with the Kübler Indices, we correlate the anchizone metamorphism of the Northern Triassic and Paleozoic units with the  $D_1$  deformation phase. Therefore, we interpret the tight-isoclinal folding observed in the Paleozoic and in the Northern Triassic unit of the Drina-Ivanjica thrust sheet as related to the latest Jurassic–earliest Cretaceous deformation event. In contrast, Djokovic (1985) interpreted the same structures as being related to a Paleozoic deformation event.

### 5.3 Implications for the Late Jurassic–Early Cretaceous evolution of the Drina-Ivanjica thrust sheet

Part of the Dinaric (Western Vardar) ophiolites probably formed in a supra-subduction setting following intra-oceanic subduction initiation (e.g. Bortolotti et al. 2005; Maffione et al. 2015). The Middle–Late Jurassic age of the metamorphic sole at the base of the ophiolitic thrust sheet(s) provides evidence for the early phases of intra-oceanic subduction (Dimo-Lahitte et al. 2001; Bortolotti et al. 2013; Šoštarić et al. 2014; Maffione et al. 2015). Intra-oceanic subduction was followed by top-WNW emplacement of the ophiolitic thrust sheet(s) onto the Adriatic passive margin (Gawlick et al. 2008, 2009; Schmid et al. 2008; Schefer 2012) leading to deformation (nappe stacking), burial and metamorphism in the Internal Dinarides. Early Cretaceous tectonometamorphic events have been reported from various locations in the Internal Dinarides such as the Kopaonik and Studenica units (supplemented by 85–110 Ma multigrain Ar/Ar ages) (Schefer 2012) as well as the Medvednica (122–111 Ma K/Ar ages and 135–122 Ar/Ar ages) (Belak et al. 1995; Borojevic et al. 2012) and the Fruška Gora (128–118 Ma K/Ar ages) (Milovanovic et al. 1995). Single grain dating of detrital white micas in the Vardar Flysch unit also yielded an Early Cretaceous age group (c.a. 105–150 Ma) (Ilic et al. 2005). Our 130–150 Ma K/Ar ages suggest a slightly older metamorphic event that affected the Paleozoic and in the

Northern Triassic unit of the Drina-Ivanjica thrust sheet. Asymmetric F1 folds imply top-WNW tectonic transport during this event in our study area which is in agreement with the direction of ophiolite obduction determined on the basis of stretching lineations and shear criteria in the sub-ophiolitic melange and in the mylonitic metamorphic sole of the ophiolites (Carosi et al. 1996; Karamata et al. 2000; Schmid et al. 2008; Schefer 2012).

Our data confirm the idea that the latest Jurassic to Early Cretaceous tectonic burial of the distal Adriatic margin (Internal Dinarides) is related to the underthrusting of the continental margin below the obducting Western Vardar ophiolites (Fig. 8). Mechanical and thermal feasibility of obduction systems have been tested by analogue (Agard et al. 2014) and numerical (Duretz et al. 2016) experiments. Such experiments suggest that underthrusting of the continental margin results in regional metamorphism in the continental rocks which is followed by exhumation. In this sense we correlate the Late Jurassic–Early Cretaceous low-grade metamorphism and associated deformation of the Drina-Ivanjica Paleozoic and the Northern Triassic unit with the underthrusting of the Adriatic margin below the Western Vardar ophiolites.

#### 5.4 Implications for the Late Cretaceous–Paleogene evolution of the Drina-Ivanjica thrust sheet

Underthrusting of the Drina-Ivanjica thrust sheet was followed by exhumation, erosion, and the deposition of the Albian–Cenomanian sedimentary succession (Pejovic and Radoicic 1971; Brkovic et al. 1977; Mojsilovic et al. 1977; Olujic and Karovic 1986) (Fig. 8). The erosional unconformity which forms the base of the Albian strata truncates the ophiolites, the sub-ophiolitic melange, and even the Southern and Northern Triassic units and the Paleozoic in the study area (Figs. 2, 7). This means that the metamorphic Paleozoic and Northern Triassic units yielding 135–150 Ma K/Ar ages were already exhumed to the surface by  $\sim 110$  Ma.

Contrary to the  $D_1$  deformation phase that only affected the Paleozoic and Northern Triassic unit of the Drina-Ivanjica thrust sheet,  $D_2$  deformation phase has also affected the Albian–Campanian transgressive succession providing further evidence for the timing of  $D_1$  and  $D_2$  events. As shown by Figs. 4b, 7, and 8, we propose that  $D_2$  structures cut across the Albian–Campanian succession. The interpretation on Fig. 7 furthermore implies that part of the displacement along the regional  $D_2$  top-NNE back-thrust took place prior or coeval to the deposition of these sediments. Consequently, the Albian–Campanian strata could be partly syn-kinematic with respect to  $D_2$  (back)thrusting in the region. However, indisputable proof

for syn- $D_2$  deposition is yet lacking, thus our interpretation has to be treated only as one possible solution.

$D_2$  deformation is characterized by brittle NE–SW shortening which resulted in the formation of map-scale NW–SE trending thrusts and fault-related folds in the study area (Figs. 2, 4, and 7). The observation of dominantly brittle folding around NW–SE trending axes is in agreement with data of previous structural works in the region (Djokovic 1985; Trivic et al. 2010) as well as with the dominant map-scale trend of contractional structures in the Dinarides (Fig. 1). The vergence of  $D_2$  thrusts and asymmetric folds indicates a top-SW tectonic transport direction in the NE part of the study area, but a top-NE tectonic transport direction in the SW part of the study area (Figs. 2, 7). A top-SW tectonic transport direction is in agreement with the prevailing tectonic transport direction in most of the Dinarides, which took place after the collision between Adria and Europe (Schmid et al. 2008; Ustaszewski et al. 2010), while the significance of the top-NE tectonic transport direction during  $D_2$  thrusting is discussed in the next chapter.

According to Ustaszewski et al. (2009) the collision between Adria and Europe (Dacia Mega-Unit) took place in Maastrichtian to earliest Paleogene times. The collision resulted in Paleogene amphibolite facies metamorphism (Ar/Ar white mica ages of 36–46 Ma) in the innermost Dinarides, south-east from our study area, and in the emplacement of the Kopaonik thrust sheet onto the Studenica thrust sheet (Schefer 2012). Following this metamorphism the Studenica thrust sheet was emplaced on top of the Drina-Ivanjica thrust sheet by a transpressive fault (Schefer 2012).

The dominantly brittle  $D_2$  structures imply that the final (latest Cretaceous–Paleogene) suturing of Adria and Europe did not result in deep tectonic burial of the Drina-Ivanjica thrust sheet (Fig. 8). Thus  $D_2$  deformation occurred at shallow crustal levels, which is in agreement with previous results (brittle thrusting and folding) from the region (Djokovic 1985; Trivic et al. 2010). Only one of our 1  $\mu\text{m}$ -fraction K/Ar samples (sample 192) yielded Paleocene age ( $\sim 61$  Ma) which is difficult to interpret due to the lack of any other samples showing similar ages. A probable solution is that this datum represents deformation or fluid flow-induced crystallization of some very-fine-grained white micas during the predominantly brittle  $D_2$  deformation phase.

#### 5.5 Origin of the Southern and Northern Triassic units

Based on our data the Late Jurassic–Early Cretaceous metamorphism and associated  $D_1$  deformation only affected the Paleozoic and the Northern Triassic unit of the

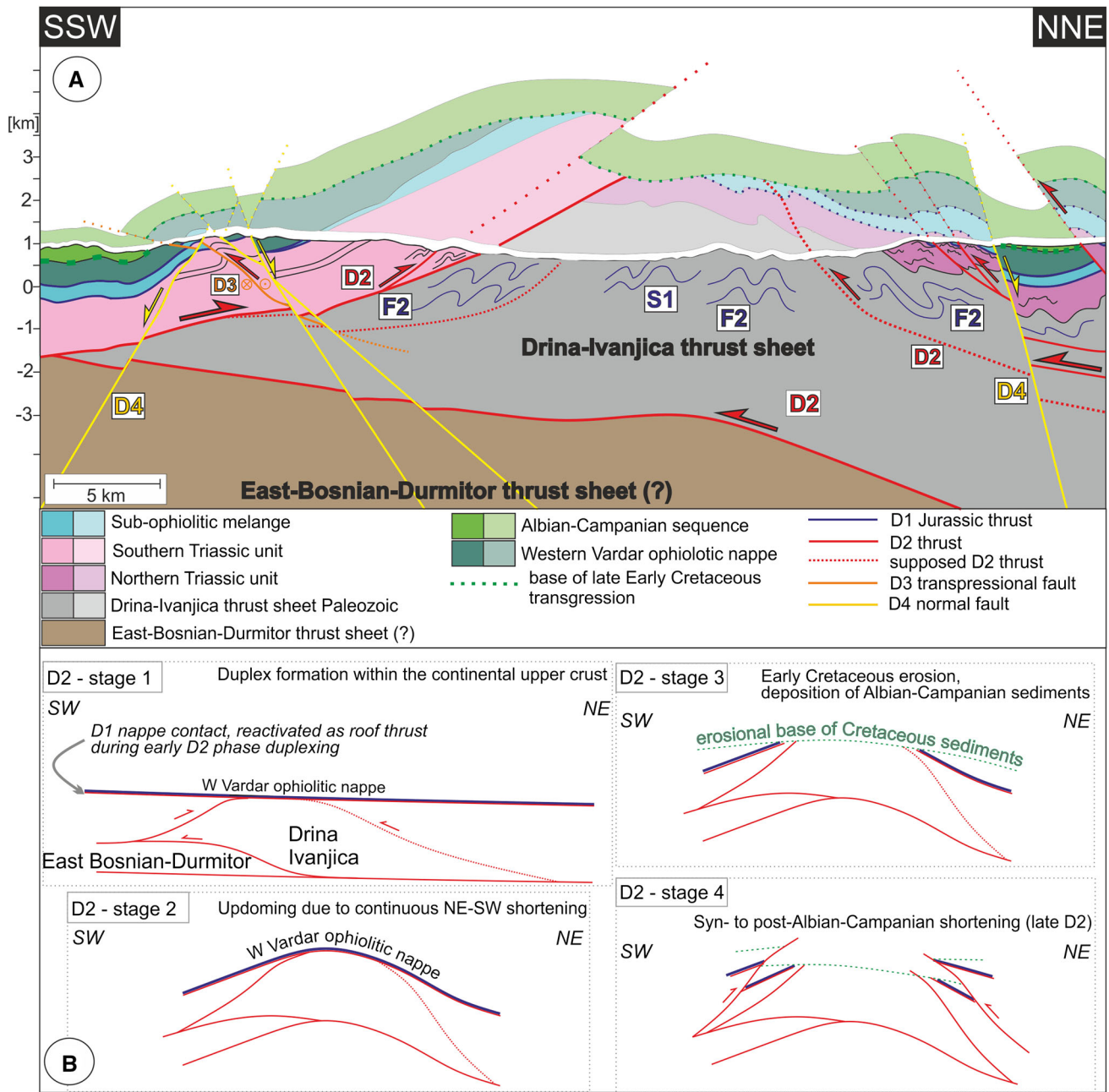


**Fig. 7 a** SSW–NNE geological cross-section across the study area showing a possible interpretation of the major tectonic features and attributed deformation phases. The trace of the section is shown on

**Fig. 7 b** Tentative model for the kinematic evolution of the Drina-Ivanjica thrust sheet and surrounding units to visualize possible explanation of structural relationships

Drina-Ivanjica thrust sheet while the Southern Triassic unit is lacking any record of D<sub>1</sub> deformation and low-grade metamorphism. Well-preserved carbonate textures and fossils (Fig. 3f) also confirm the absence of significant crystal plastic deformation. Therefore, we suggest that the Southern Triassic unit might not be the original sedimentary cover of the Drina-Ivanjica Paleozoic and thus be different from the Northern Triassic. This idea/assumption contradicts previous works which all have assumed a

stratigraphic contact between the Paleozoic and the Southern Triassic unit (Brkovic et al. 1977; Mojsilovic et al. 1977; Olujic and Karovic 1986; Chiari et al. 2011). In contrary, the Northern Triassic unit shares the tectonic history of the Drina-Ivanjica Paleozoic. Hence we suggest that the Northern Triassic unit is the original sedimentary cover of the Drina-Ivanjica Paleozoic (Figs. 7, 8).

Considering the lack of Late Jurassic–Early Cretaceous low-grade metamorphism in the Southern Triassic unit, we

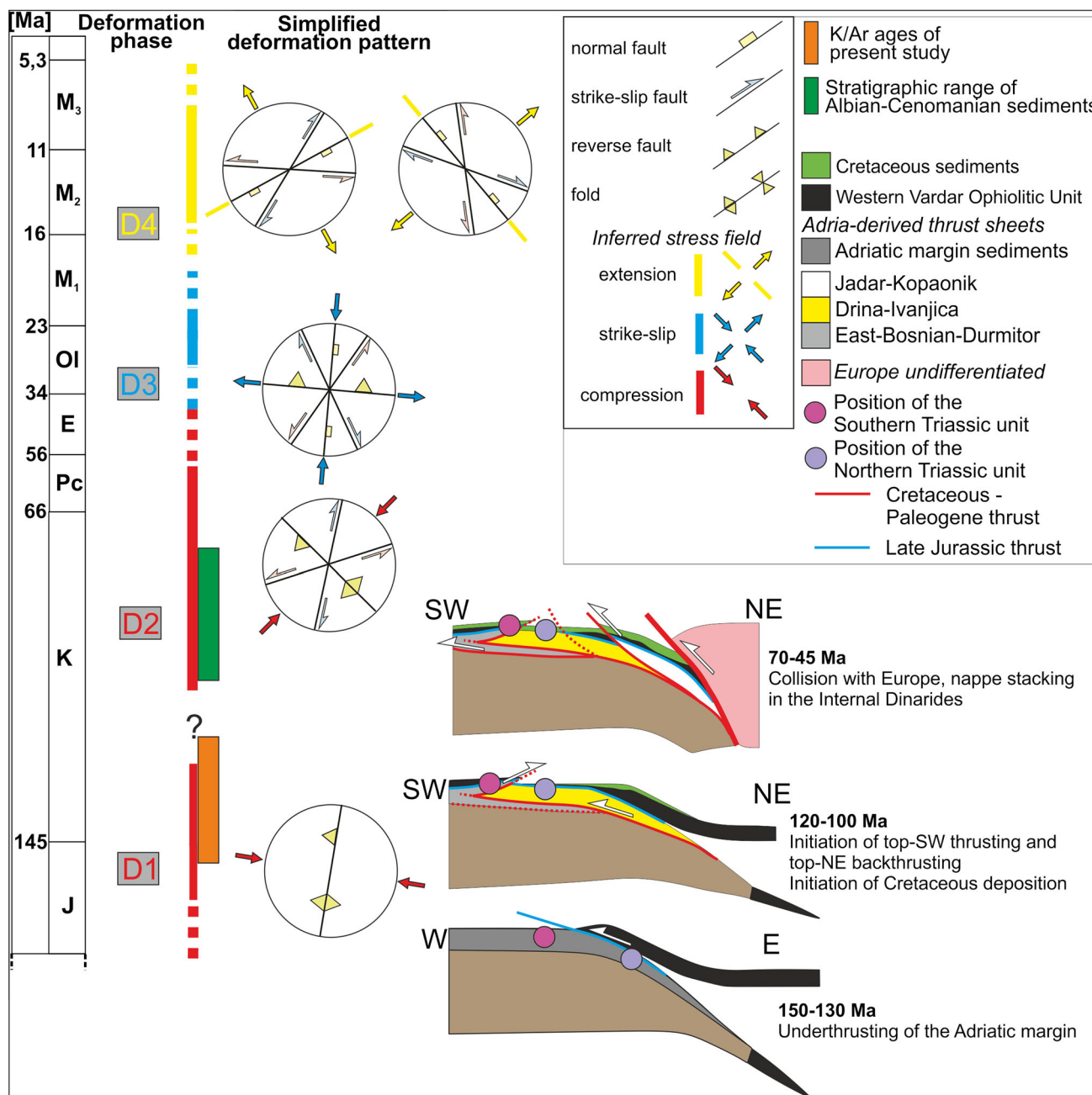


**Fig. 8** Summary of the Jurassic-Neogene deformation history of the study area. Stereoplots of the simplified deformation patterns show the approximate stress field and related structures through time.

cannot correlate it with the innermost thrust sheets of the Internal Dinarides (Jadar-Kopaonik thrust sheet) since this thrust sheet experienced Cretaceous–Paleogene metamorphism (e.g. Schmid et al. 2008; Schefer 2012). Such a non-metamorphic Triassic succession is more likely to have originated from a more external thrust sheet of the Dinarides, possibly from the East Bosnian-Durmitor thrust sheet, which is in the footwall of the Drina-Ivanjica thrust sheet and is found on surface to the SW from our study area

Large-scale schematic sections show our model for the Jurassic-Paleogene tectonic evolution of the studied part of the Internal Dinarides in three steps

(Schmid et al. 2008) (Fig. 8). However, an exact attribution of the Southern Triassic to the East Bosnian-Durmitor thrust sheet requires further analysis. Common occurrence of NE-verging  $D_2$  thrust faults, asymmetric  $F_2$  folds and fault-related folds near the contact of the Paleozoic and the Southern Triassic unit (Figs. 2, 4, and 7) also support the southwestern origin of the Southern Triassic unit. Previous works attributed the NE-verging folds to the formation of the Drina-Ivanjica anticline, assuming that the Triassic

successions on both sides of the Paleozoic belong to the one and the same tectonic unit (Milovanovic 1984; Djokovic 1985; Chiari et al. 2011). However, this model lacks an explanation of the observed structures.

As an alternative, we suggest that the Northern and Southern Triassic units are of different origin and the NE-verging  $D_2$  structures are related to a regional-scale  $D_2$  backthrusting event (Figs. 7, 8). Such a structure could explain both the commonly found NNE-verging structures (Figs. 2, 4, and 7) in the proximity of the contact between the Paleozoic and the Southern Triassic unit and the lack of low-grade metamorphism in latter. Displacement along the backthrust might have taken place before the Albian onset of sedimentation and partly after its termination in the Campanian (Figs. 7 and 8) although evidence for syn- $D_2$  deposition for the Albian-Campanian formations is yet lacking.

It is also possible that the suggested NE-vergent backthrusting was coeval with and connected to the general post-obduction SW-vergent thrusting and formed a sort of triangle-zone. In this way, the Drina-Ivanjica thrust sheet would disrupt the East-Bosnian-Durmitor unit, having part of it as footwall and part of it as hanging wall (Figs. 7, 8). In this context, backthrusting would have been part of the general southwest-ward displacement, just accommodating the shortening with an opposite vergence. Such geometry has not been documented in the Dinarides, but for instance, it was suggested for the Silica unit of the Western Carpathians (Schmid et al. (2008)). A possible kinematic solution is shown by Fig. 7b suggesting that the  $D_1$  nappe contact at the base of the Western Vardar ophiolites might have reactivated as a roof thrust during early  $D_2$  backthrusting thus accommodating the displacement of the Southern Triassic. Such a roof thrust would also explain why large-scale repetition of the Western Vardar ophiolites is not observed in the region. The assumed minor (roughly 2 km) displacement of the Albian-Campanian sediments (Fig. 7a) is related to the post-Campanian displacement (reactivation) along the backthrust (late  $D_2$  phase).

## 5.6 Implications concerning the Late-Paleogene to Miocene tectonic evolution

NE-SW shortening during  $D_2$  deformation was followed by strike-slip movements ( $D_3$ ), which in most cases cut, but in some cases possibly link to  $D_2$  thrust faults (Figs. 2, 7a). Stress tensor calculations and the trend of map-scale structures both imply roughly N-S compression, and subordinate perpendicular extension (Fig. 5). Though the stress regime changed from pure compression of  $D_2$  to transpression of  $D_3$ , the shortening directions of the two phases do not differ significantly from each other (NE-SW and N-S). The age of  $D_3$  strike-slip movements has a

possible upper limit, since Miocene formations seem to seal  $D_3$  strike-slip faults (Fig. 2a), however satisfying evidences are lacking. Direct evidence for the lower limit is lacking due to the absence of Paleogene rocks in the study area. However we speculate using an indirect argument for the lower limit on the basis of regional forcing factors. It has been shown that indentation tectonics and related shortening in the Alps resulted in lateral wrenching in the Dinarides and the development of NW-SE striking dextral systems parallel to the Dinaridic orogen (e.g. Picha 2002; Van Gelder et al. 2017). Ilic and Neubauer (2005) also attributed the Oligocene-Early Miocene transpression (NE-SW compression and perpendicular extension based on data from the Central Dinarides) to orogen-parallel movements induced by the Adriatic indentation. NNW-SSE transpression assigned to the Oligocene was also reported from the Kopaonik region (Mladenovic et al. 2015). The transition from thrusting in the Italian Alps into strike-slip faulting in Slovenia is also well-documented and is possibly linked to the strike-slip faulting in the Central Dinarides (Vrabec and Fodor 2006). Our data of  $D_3$  strike-slip movements are probably the result of the same driving forces. However, further research is needed to explain the mechanisms of Paleogene-Miocene lateral wrenching in the central Dinarides.

Strike-slip movements were followed by extension ( $D_4$ ) as evidenced by overprinting relations between NE-SW and NW-SE trending normal faults and  $D_3$  strike slip faults (Figs. 2 and 7a). We have distinguished two extensional stress tensor groups that represent orogen-parallel (NW-SE) and orogen-perpendicular (NE-SW) extension (Fig. 5). Our observations and the dataset are not sufficient for determining the relative chronology between orogen-parallel and orogen-perpendicular extension. These might also be partly coeval having formed in a multidirectional extensional stress field. These results are in agreement with a paleostress study reporting Early Miocene orogen-perpendicular (NE-SW) and Middle Miocene orogen-parallel (NW-SE) extensional phases from the Central Dinarides (Ilic and Neubauer 2005). Similar extensional directions were documented in the Valjevo region as well (Gerzina and Csontos 2003; Mladenovic et al., 2014). Andric et al. (2017) also observed several syn-sedimentary extensional episodes, with similar stress axes, in the Neogene Sarajevo basin. Neogene extension in the Dinaric orogen is probably driven by slab-rollback processes of the Carpathian-Dinaridic realm. Thus it could be linked either to the roll-back of the Carpathian slab which also created space for the extruding nappes derived from the Alps (Ratschbacher et al. 1989; Fodor et al. 1998; Horváth et al. 2006), and/or to the rollback of the Dinaric slab (Matenco and Radivojevic 2012; Toljic et al. 2013; Handy et al. 2015; Le Breton et al. 2017).

## 6 Concluding remarks

We applied multi-scale structural analysis, Illite Crystallinity measurements, and K/Ar dating in order to trace the record of obduction and collision processes in part of the Internal Dinarides in Western Serbia. This integrated approach allowed us to distinguish between structures related to Late Jurassic–Early Cretaceous underthrusting of the Drina-Ivanjica thrust sheet below the obducted Western Vardar ophiolites and to the latest Cretaceous–Paleogene collision between Adria and Europe. Our most important findings are:

1. Ductile deformation (D<sub>1</sub>) and very low-grade metamorphism in the Drina-Ivanjica Paleozoic and in the Northern Triassic unit was probably related to the Late Jurassic–Early Cretaceous top-WNW obduction of the Western Vardar ophiolites.
2. The Northern Triassic unit shares the same deformation history with the Drina-Ivanjica Paleozoic and yields similar KI and K/Ar values as the latter unit. Therefore, we suggest that the Northern Triassic unit is the original sedimentary cover of the Drina-Ivanjica Paleozoic.
3. The Southern Triassic unit has not been affected by D<sub>1</sub> ductile deformation and Late-Jurassic–Early Cretaceous low-grade metamorphism, therefore it might not represent the sedimentary cover of the Drina-Ivanjica Paleozoic. We propose that this unit might have originated from a more external Dinaridic thrust sheet, most likely from the East Bosnian–Durmitor thrust sheet, and having been transported to its present-day position by a top-NE backthrust (D<sub>2</sub>).
4. Latest Cretaceous–Paleogene collision between Adria and Europe is reflected in a brittle NE–SW shortening event in the study area as evidenced by map-scale D<sub>2</sub> thrust faults and abundant F<sub>2</sub> folds.
5. Late Paleogene to earliest Miocene tectonics of the region was characterized by map-scale strike-slip faults (D<sub>3</sub>), which accommodated N–S shortening and perpendicular extension. These faults are cut by Miocene normal faults (D<sub>4</sub>) that accommodated both orogen-parallel and orogen-perpendicular extension.

**Acknowledgement** The study was supported by the Hungarian National Research Found (OTKA) 113013 and by Ministry of Education Science and Technological Development of the Republic of Serbia, Project No. 176015. The K–Ar studies were supported by the Bolyai Research Scholarship of the Hungarian Academy of Sciences to Zsolt Benkó (BO/442/16). Finally, we thank the two anonymous reviewers and editors for substantially improving our manuscript with their constructive remarks.

**Open Access** This article is distributed under the terms of the Creative Commons Attribution 4.0 International License (<http://creativecommons.org/licenses/by/4.0/>), which permits unrestricted use, distribution, and reproduction in any medium, provided you give appropriate credit to the original author(s) and the source, provide a link to the Creative Commons license, and indicate if changes were made.

## References

- Abad, I. (2007). Physical meaning and applications of the illite Kübler index: measuring reaction progress in low-grade metamorphism. *Diagenesis and Low-Temperature Metamorphism, Theory, Methods and Regional Aspects, Seminarios. Sociedad Espanola: Sociedad Espanola Mineralogia* (pp. 53–64).
- Agard, P., Zuo, X., Funicello, F., Bellahsen, N., Faccenna, C., & Savva, D. (2014). Obduction: why, how and where. Clues from analog models. *Earth and Planetary Science Letters*, 393, 132–145.
- Andrić, N., Sant, K., Matenco, L., Mandić, O., Tomljenović, B., Pavelić, D., et al. (2017). The link between tectonics and sedimentation in asymmetric extensional basins: Inferences from the study of the Sarajevo-Zenica Basin. *Marine and Petroleum Geology*, 83, 305–332.
- Angelier, J. (1984). Tectonic analysis of fault slip data sets. *Journal of Geophysical Research: Solid Earth*, 89(B7), 5835–5848.
- Árkai, P., Balogh, K., & Dunkl, I. (1995). Timing of low-temperature metamorphism and cooling of the Paleozoic and Mesozoic formations of the Bükkium, innermost Western Carpathians, Hungary. *Geologische Rundschau*, 84(2), 334–344.
- Árkai, P., & Ghabrial, D. S. (1997). Chlorite crystallinity as an indicator of metamorphic grade of low-temperature metaigneous rocks; a case study from the Bükk Mountains, Northeast Hungary. *Clay Minerals*, 32(2), 205–222.
- Balogh, K. (1985). K/Ar dating of Neogene volcanic activity in Hungary: Experimental technique, experiences and methods of chronological studies. *ATOMKI Közlemények*, 27(3), 277–288.
- Bazylev, B., Popević, A., Karamata, S., Kononkova, N., Simakin, S., Olujić, J., et al. (2009). Mantle peridotites from the Dinaridic ophiolite belt and the Vardar zone western belt, central Balkan: A petrological comparison. *Lithos*, 108(1), 37–71.
- Belak, M., Jamičić, D., Crnko, J., & Sremac, J. (1995). *Low-metamorphic rocks from the lower part of Bliznac creek* (pp. 97–102). Zagreb: Geological guide of Mts. Medvednica. Naftaplin.
- Bernoulli, D., & Laubscher, H. (1972). The palinspastic problem of the Hellenides. *Eclogae Geologicae Helveticae*, 65(1), 107.
- Borojević, Š. S., Franz, N., & Robert, H. (2012). Tectonothermal history of the basement rocks within the NW Dinarides: New<sup>40</sup>Ar/<sup>39</sup>Ar ages and synthesis. *Geologica Carpathica*, 63(6), 441–452.
- Bortolotti, V., Chiari, M., Marroni, M., Pandolfi, L., Principi, G., & Saccani, E. (2013). Geodynamic evolution of ophiolites from Albania and Greece (Dinaric-Hellenic belt): One, two, or more oceanic basins? *International Journal of Earth Sciences*, 102(3), 783–811.
- Bortolotti, V., Kodra, A., Marroni, M., Mustafa, F., Pandolfi, L., Principi, G., et al. (1996). Geology and petrology of ophiolitic sequences in the Mirdita region (Northern Albania). *Ophioliti*, 21(1), 3–20.
- Bortolotti, V., Marroni, M., Pandolfi, L., & Principi, G. (2005). Mesozoic to Tertiary tectonic history of the Mirdita ophiolites, northern Albania. *Island Arc*, 14(4), 471–493.
- Brković, T., Malešević, M., Klisić, M., Urošević, M., Trifunović, S., Radovanović, Z., et al. (1977). *Basic Geological Map of Former*



- Yugoslavia 1:100000, Sheet Čačak*. Belgrade: Institute for Geological and Geophysical Research. (in Serbian).
- Osnovna Geološka Karta SFRJ, Geological maps of former Yugoslavia, 1:100.000: *Beograd, Savezni Geoloski Zavod*.
- Carosi, R., Cortesogno, L., Gaggero, L. T., & Marroni, M. (1996). Geological and petrological features of the metamorphic sole from the Mirdita nappe, northern Albania. *Ophioliti*, 21(1), 21–40.
- Chiari, M., Djerić, N., Garfagnoli, F., Hrvatović, H., Krstić, M., Levi, N., et al. (2011). The geology of the Zlatibor-Maljen area Western Serbia: A geotraverse across the ophiolites of the Dinaric-Hellenic collisional belt. *Ophioliti*, 36(2), 139–166.
- Csontos, L., Gerzina, N., Hrvatović, H., Schmidt, S., and Tomljenović, B., Structural evolution of the Internal Dinarides: a preliminary study based on selected regions, in Proceedings Procc. 5 th International Symposium on Eastern Mediterranean Geology2004, p. 377–380.
- Dilek, Y., 2008, Geochemistry of the Jurassic Mirdita Ophiolite (Albania) and the MORB to SSZ evolution of a marginal basin oceanic crust: *Lithos*, 100, 1–4, 174–209.
- Dilek, Y., Furnes, H., & Shallo, M. (2007). Suprasubduction zone ophiolite formation along the periphery of Mesozoic Gondwana. *Gondwana Research*, 11(4), 453–475.
- Dimitrijević, M. (1982). Dinarides: an outline of the tectonics. *Earth Evol Sci*, 1, 4–23.
- Dimo-Lahitte, A., Monié, P., and Vergély, P., 2001, Metamorphic soles from the Albanian ophiolites: Petrology, 40Ar/39Ar geochronology, and geodynamic evolution: *Tectonics*, 20, 1, 78–96.
- Djerić, N., Gerzina, N., and Schmid, S. M., 2007, Age of the Jurassic radiolarian chert formation from the Zlatar mountain (SW Serbia): *Ophioliti*, 32, 2, 101–108.
- Djoković, I., 1985, the use of structural analysis in determining the fabric of Palaeozoic formations in the Drina-Ivanjica region: *Geološki anali balkanskoga poluostrva*, 49, 11–160.
- Duret, T., Agard, P., Yamato, P., Ducassou, C., Burov, E. B., & Gerya, T. V. (2016). Thermo-mechanical modeling of the obduction process based on the Oman ophiolite case. *Gondwana Research*, 32, 1–10.
- Ercegovic, M. (1975). Microspores of the older Paleozoic from W: Serbia. *Belgrade: Séances Soc. Serbe Géol*, 17–20.
- Fodor, L., Jelen, B., Márton, E., Skaberne, D., Čar, J., & Vrabec, M. (1998). Miocene-Pliocene tectonic evolution of the Slovenian Periadriatic fault: implications for Alpine-Carpathian extrusion models. *Tectonics*, 17(5), 690–709.
- Frey, M. (1970). The step from diagenesis to metamorphism in pelitic rocks during Alpine orogenesis. *Sedimentology*, 15(3–4), 261–279.
- Gawlick, H.-J., Frisch, W., Hoxha, L., Dumitrica, P., Krystyn, L., Lein, R., et al. (2008). Mirdita Zone ophiolites and associated sediments in Albania reveal Neotethys Ocean origin. *International Journal of Earth Sciences*, 97(4), 865–881.
- Gawlick, H.-J., Sudar, M., Suzuki, H., Deric, N., Missoni, S., Lein, R., et al. (2009). Upper Triassic and Middle Jurassic radiolarians from the ophiolitic mélange of the Dinaridic Ophiolite Belt. *SW Serbia: Neues Jahrbuch für Geologie und Paläontologie-Abhandlungen*, 253(2–3), 293–311.
- Gerzina, N., & Csontos, L. (2003). Deformation sequence in the Vardar Zone: surroundings of Jadar Block; Serbia: *Ann. Univ. Sci. Budapestinensis. Sect. Geol*, 35, 139–140.
- Goffé, B., Michard, A., Kienast, J. R., & Le Mer, O. (1988). A case of obduction-related high-pressure, low-temperature metamorphism in upper crustal nappes. *Arabian continental margin, Oman: PT paths and kinematic interpretation: Tectonophysics*, 151(1–4), 363–386.
- Handy, M. R., Ustaszewski, K., and Kissling, E., 2015, Reconstructing the Alps–Carpathians–Dinarides as a key to understanding switches in subduction polarity, slab gaps and surface motion: *International Journal of Earth Sciences*, 104, 1, 1–26.
- Horváth, F., Bada, G., Szafián, P., Tari, G., Ádám, A., & Cloetingh, S. (2006). Formation and deformation of the Pannonian Basin: constraints from observational data: *Geological Society. London, Memoirs*, 32(1), 191–206.
- Hunziker, J., Frey, M., Clauer, N., & Dallmeyer, R. (1987). Reply to the comments on the evolution of illite to muscovite by JR Glasman. *Contributions to Mineralogy and Petrology*, 96(1), 75–77.
- Ilić, A., & Neubauer, F. (2005). Tertiary to recent oblique convergence and wrenching of the Central Dinarides: constraints from a palaeostress study. *Tectonophysics*, 410(1), 465–484.
- Ilic, A., Neubauer, F., and Handler, R., 2005, Late Paleozoic–Mesozoic tectonics of the Dinarides revisited: Implications from 40Ar/39Ar dating of detrital white micas: *Geology*, 33, 3, 233–236.
- Jolivet, L., Faccenna, C., Agard, P., Frizon de Lamotte, D., Menant, A., Sternai, P., and Guillocheau, F., 2015, Neo-Tethys geodynamics and mantle convection: from extension to compression in Africa and a conceptual model for obduction 1: *Canadian Journal of Earth Sciences*, 53, 11, 1190–1204.
- Karamata, S. (2006). The geodynamical framework of the Balkan Peninsula: its origin due to the approach, collision and compression of Gondwanian and Eurasian units: *Tectonic Development of the Eastern Mediterranean Region. Geological Society, London, Special Publication*, 260, 155–178.
- Karamata, S., and Krstić, B., 1996, Terranes of Serbia and neighbouring areas: *terranes of Serbia*, 25–40.
- Karamata, S., Korikovskiy, S., and Kurdyukov, E., Prograde contact metamorphism of mafic and sedimentary rocks in the contact aureole beneath the Brezovica harzburgite Massif, in Proceedings Geology and Metallogeny of the Dinarides and the Vardar zone. Proceedings of the International Symposium. Academy of Science & Arts of the Republic of Srpska, Collections & Monographs, Department of Natural, Mathematical & Technical Science2000, Volume 1, p. 171–178.
- Kovács, S., Sudar, M., Grđinaru, E., Karamata, S., Gawlick, H., HAAS, J., PÉRO, C., GAETANI, M., Mello, J., and POLÁK, M., 2011, Triassic evolution of the tectonostratigraphic units of the Circum-Pannonian Region: *Jahrbuch der Geologischen Bundesanstalt*, 151, 3–4, 199–280.
- Kubat, I., Reljić, D., Veljković, D., Strajin, V., Begić, F., Dimitrov, P., et al. (1976). *Basic Geological Map of Former Yugoslavia 1:100000*. Institute for Geology Sarajevo and Federal Geologic Survey, Belgrade (in Serbian): Sheet Ljubovija.
- Kübler, B., 1966, La cristallinité de l'illite et les zones tout à fait supérieures du métamorphisme: *In: Etages tectoniques. – Univ. Neuchâtel, Inst. Geol.*, 105–122.
- Kübler, B. (1968). Evaluation quantitative du métamorphisme par la cristallinité de l'illite. *Bulletin Centre Recherche Pau SNPA*, 2, 385–397.
- Le Breton E, Handy MR, Molli G, Ustaszewski K (2017) Post-20 Ma Motion of the Adriatic Plate: New Constraints From Surrounding Orogens and Implications for Crust-Mantle Decoupling. *Tectonics*
- Maffione, M., Thieulot, C., Van Hinsbergen, D. J., Morris, A., Plümpner, O., & Spakman, W. (2015). Dynamics of intraoceanic subduction initiation: 1. *Oceanic detachment fault inversion and the formation of supra-subduction zone ophiolites: Geochemistry, Geophysics, Geosystems*, 16(6), 1753–1770.
- Matenco, L., & Radivojević, D. (2012). On the formation and evolution of the Pannonian Basin: constraints derived from the structure of the junction area between the Carpathians and Dinarides. *Tectonics*, 31, 6.

- Milovanović, D. (1984). Petrology of low metamorphosed rocks of the central part of the Drina-Ivanjica Paleozoic: *Bull. Mus. Hist. Nat. Belgrade*, *A*, *39*, 13–139.
- Milovanovic, D., Marchig, V., and Stevan, K., 1995, Petrology of the crossite schist from Fruška Gora Mts (Yugoslavia), relic of a subducted slab of the Tethyan oceanic crust: *Journal of Geodynamics*, *20*, *3*, 289–304.
- Mladenovic, A., Trivic, B., Cvetkovic, V., and Pavlovic, R., A brittle tectonic history of the Internal Dinarides: an inference based on the paleostress study in the Valjevo area (western Serbia), in Proceedings EGU General Assembly Conference Abstracts2014, Volume 16, p. 46.
- Mladenović, A., Trivić, B., and Cvetković, V., 2015, How tectonics controlled post-collisional magmatism within the Dinarides: Inferences based on study of tectono-magmatic events in the Kopaonik Mts.(Southern Serbia): *Tectonophysics*, *646*, 36–49.
- Mojsilović, S., Baklajić, D., & Djoković, I. (1977). *Basic Geological Map of Former Yugoslavia 1:100000, Sheet Titovo Užice*. Belgrade: Institute for Geological and Geophysical Research. (in Serbian).
- Mojsilović, S., Filipović, I., Baklajić, D., Đoković, I., & Navala, M. (1972). *Basic Geological Map of Former Yugoslavia 1:100000*. Federal Geological Survey, Belgrade (in Serbian): Sheet Valjevo.
- Olujić, J., Karović, J. (1986). Basic Geological Map of Former Yugoslavia 1:100000, Sheet Višegrad, “Geoinženjering” - Institute for Geology Sarajevo and Federal Geologic Survey, Belgrade (in Serbian)
- Pejović, D., and Radoičić, R., 1971, Über die stratigraphie der Kreide serie der Mokra Gora: *Bulletin Scientifique du Conseil des Academies des Sciences et des arts de la RSF de Yugoslavie, Sect. A*, *16*, 7-8-138.
- Picha, F. J. (2002). Late orogenic strike-slip faulting and escape tectonics in frontal Dinarides-Hellenides. *Croatia, Yugoslavia, Albania, and Greece: AAPG bulletin*, *86*(9), 1659–1671.
- Ratschbacher, L., Frisch, W., Neubauer, F., Schmid, S., & Neugebauer, J. (1989). Extension in compressional orogenic belts: the eastern Alps. *Geology*, *17*(5), 404–407.
- Roberson, H. E., & Lahann, R. W. (1981). Smectite to illite conversion rates: effects of solution chemistry. *Clays and Clay Minerals*, *29*(2), 129–135.
- Robertson, A. (2004). Development of concepts concerning the genesis and emplacement of Tethyan ophiolites in the Eastern Mediterranean and Oman regions. *Earth-Science Reviews*, *66*(3), 331–387.
- Schefer, S., 2012, Tectono-metamorphic and magmatic evolution of the Internal Dinarides (Kopaonik area, southern Serbia) and its significance for the geodynamic evolution of the Balkan Peninsula: University of Basel.
- Schmid, S. M., Bernoulli, D., Fügenschuh, B., Matenco, L., Schefer, S., Schuster, R., Tischler, M., and Ustaszewski, K., 2008, The Alpine-Carpathian-Dinaridic orogenic system: correlation and evolution of tectonic units: *Swiss Journal of Geosciences*, *101*, *1*, 139–183.
- Šošarić, S. B., Palinkaš, A., Neubauer, F., Cvetković, V., Bernroider, M., & Genser, J. (2014). The origin and age of the metamorphic sole from the Rogozna Mts., Western Vardar Belt: new evidence for the one-ocean model for the Balkan ophiolites. *Lithos*, *192*, 39–55.
- Spray, J., Bébien, J., Rex, D., & Roddick, J. (1984). Age constraints on the igneous and metamorphic evolution of the Hellenic-Dinaric ophiolites: *Geological Society. London, Special Publications*, *17*(1), 619–627.
- Steiger, R. H., & Jäger, E. (1977). Subcommittee on geochronology: convention on the use of decay constants in geo-and cosmochronology. *Earth and Planetary Science Letters*, *36*(3), 359–362.
- Toljić, M., Matenco, L., Ducea, M. N., Stojadinović, U., Milivojević, J., & Đerić, N. (2013). The evolution of a key segment in the Europe-Adria collision: the Fruška Gora of northern Serbia. *Global and Planetary Change*, *103*, 39–62.
- Tomljenović, B., Csontos, L., Márton, E., & Márton, P. (2008). Tectonic evolution of the northwestern Internal Dinarides as constrained by structures and rotation of Medvednica Mountains. *North Croatia: Geological Society, London, Special Publications*, *298*(1), 145–167.
- Trivić, B., Cvetković, V., Smiljanić, B., and Gajić, R., 2010, Deformation pattern of the palaeozoic units of the Tethyan suture in the central Balkan Peninsula: a new insight from study of the Bukulja-Lazarevac Palaeozoic unit (Serbia): *Ofioliti*, *35*, *1*, 21–32.
- Ustaszewski, K., Kounov, A., Schmid, S. M., Schaltegger, U., Krenn, E., Frank, W., et al. (2010). Evolution of the Adria-Europe plate boundary in the northern Dinarides: from continent-continent collision to back-arc extension. *Tectonics*, *29*, 6.
- Ustaszewski, K., Schmid, S. M., Lugović, B., Schuster, R., Schaltegger, U., Bernoulli, D., Hottinger, L., Kounov, A., Fügenschuh, B., and Schefer, S., 2009, Late Cretaceous intra-oceanic magmatism in the internal Dinarides (northern Bosnia and Herzegovina): Implications for the collision of the Adriatic and European plates: *Lithos*, *108*, *1*, 106–125.
- Van Gelder, I., Willingshofer, E., Sokoutis, D., & Cloetingh, S. (2017). The interplay between subduction and lateral extrusion: a case study for the European Eastern Alps based on analogue models. *Earth and Planetary Science Letters*, *472*, 82–94.
- Voll, G. (1976). Recrystallization of quartz, biotite and feldspars from Erstfeld to the Leventina Nappe. *Swiss Alps, and its geological significance: Schweizerische mineralogische und petrographische Mitteilungen*, *56*(641), i47.
- Vrabec, M., & Fodor, L. (2006). Late Cenozoic tectonics of Slovenia: structural styles at the Northeastern corner of the Adriatic microplate. *The Adria microplate: GPS geodesy, tectonics and hazards* (pp. 151–168). Dordrecht: Springer.